NJC

Loading of chromenones on superparamagnetic iron oxide–modified dextran core–shell nanoparticles. Openness to bind to β–cyclodextrin and DNA

Journal:	*New Journal of Chemistry*
Manuscript ID:	NJ-ART-04-2015-000921.R1
Article Type:	Paper
Date Submitted by the Author:	24-Jun-2015

Complete List of Authors:	Enoch, Israel; Karunya University, Chemistry; Karunya University, Chemistry Yousuf, Sameena; Karunya University, Chemistry Selvakumar, P.; Karunya University, Chemistry Premnath, D; Karunya University, Bio-Informatics

Loading of chromenones on superparamagnetic iron oxide–modified dextran core–shell nanoparticles. Openness to bind to β–cyclodextrin and DNA†

Sameena Yousuf,[1]* Israel VMV Enoch,[1,2]* Paulraj Mosae Selvakumar,[1] Dhanaraj Premnath[3]

This paper presents the loading of chromenones viz., flavanone, hesperetin, naringenin, coumarin 6 and coumarin 7 onto aminoethylamino–modified dextran–coated superparamagnetic iron oxide core–shell nanoparticles. The chemically modified iron oxide core–shell nanoparticles retain their superparamagnetic behaviour even on chromenones loading. The accessibility of loaded chromenones by DNA for binding is analysed using UV–Visible absorption and fluorescence spectroscopy. β–cyclodextrin is used as an aid to detect whether the chromenones are buried inside the aminoethylamino–modified dextran–coated superparamagnetic iron oxide core–shell nanoparticles shell or available on the surface to readily bind to the macromolecular target. The stoichiometry of the loaded chromenones with β–cyclodextrin inclusion complex is 1:1 in all the cases, except naringenin which binds to two β–cyclodextrin molecules. Coumarin 7 shows a fluorescence quenching on binding to calf thymus DNA. The study could improve the understanding of the mode of binding of small molecules loaded on magnetic nanoparticles to DNA.

---

[1]*Department of Chemistry,* [2]*Department of Nanosciences & Technology,* [3]*Department of Bioinformatics, Karunya University, Coimbatore – 641 114, Tamil Nadu, India. Tel.: +91–9486891717. E–mails: sameen_y@yahoo.co.in; drisraelenoch@gmail.com*

† Electronic supplementary information (ESI) available: IR spectral, XPS, EDX, and XRD data for all compounds, fluorescence spectra of binding titrations, and molecular docking. For ESI see .....

Introduction

Drug delivery using iron oxide nanoparticles (NPs) depends on the possible directed transport of them into tumor cells.[1] Biocompatible superparamagnetic iron oxide nanoparticles (SPIONs) with proper surface architecture and conjugated targeting ligands have attracted a great deal of attention for drug delivery application.[2] The idea of loading small molecules onto the chemically modified SPIONs and their interaction with DNA can be utilized for the delivery of them into cancer cells, by direction using an external magnetic field. Loading small molecules on SPIONs can overcome the systemic distribution and non–specificity of anti–cancer drugs. Surface modification by dextran exhibits pH–dependent anti–oxidant properties and selectively protects normal cells from free radicals, leaving out cancer cells. It prevents the aggregation of SPIONs and limits the non–specific adsorption of biomolecules.[3] Magnetic NPs coated with amino end group–carrying dextran show greater in–vitro cellular uptake than unmodified dextran–coated SPIONs.[4] Moreover, amination of dextran renders it to get viability to easily get conjugated with chemical groups.[5] These bound micro aggregates can be characterized using their fluorescence and light scattering properties.[6] This kind of micro-aggregation can also be detected and the chemotherapeutic agent–treated–DNA of tumor can be imaged and treated if fluorescent pharmaceutically active small molecules are attached to SPIONs. The study on the binding of chemically modified SPIONs bound small molecules to DNA needs attention in order to understand the binding strength persuading with small molecules for their interaction with DNA.

Directing a drug to the required site of action, targeting a specific receptor without undesired interactions at other sites, and controlled release of drugs can be achieved by the formation of inclusion complexes with β–cyclodextrin (β–CD).[7, 8] The apparent binding constant and the mode of binding of the uncovered small molecules is modified due to the binding with tapered–cone shaped cyclic oligosaccharide, β–CD.[9, 10] The encapsulation by β–CD renders the unblocked moiety of small molecules free, allowing their interaction with DNA. Procedures leading to the binding of chromenones (CHRs) such as 2-phenyl-2,3-

dihydro-4*H*-chromen-4-one (Flavanone, PC), 5,7-dihydroxy-2-(3-hydroxy-4-methoxyphenyl)-2,3-dihydro-4*H*-chromen-4-one (Hesperetin, DC), 5,7-dihydroxy-2-(4-hydroxyphenyl)-2,3-dihydro-4*H*-chromen-4-one (Naringenin, DHC), 3-(1,3-benzothiazol-2-yl)-7(diethylamino)-2*H*-chromen-2-one (Coumarin 6, BTC), 3-(1*H*-benzimidazol-2-yl)-7-(diethylamino)-2*H*-chromen-2-one (Coumarin 7, BIC) (SI 1) to β–CD/ calf thymus DNA (ctDNA) have been well documented.[11–15] The present work is focused on (i) the loading of the CHRs onto aminoethylamino–modified dextran–coated SPIONs (CHR–SPIONs) and their binding to ctDNA, and (ii) the efficiency of encapsulation of CHRs conjugated to SPIONs by β–CD, in order to comprehend the extent of openness of the CHRs for binding to DNA. The schematic representation on the strategy of the conjugation of chromenones onto chemically modified SPIONs and their binding to targets is given in Fig. 1.

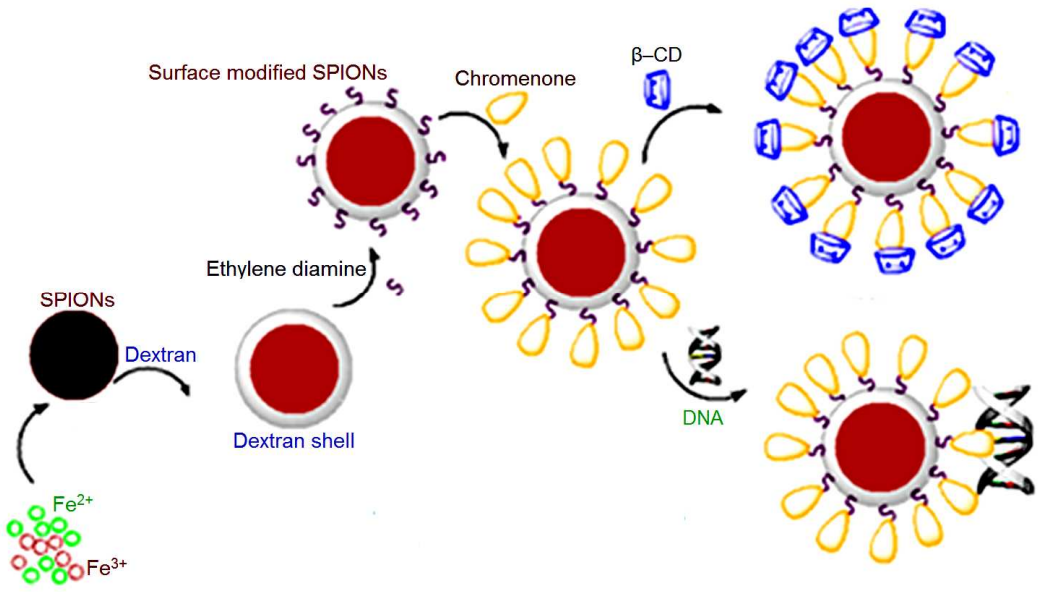

Fig. 1 Schematic representation of the conjugation of chromenones onto chemically modified SPIONs and their binding to targets.

Experimental

Preparation of test solutions

ctDNA, (Genei, Merck, India) was used without further purification. It was dissolved in NaCl solution of 50 × 10^{-3} mol dm^{-3} prior to use to obtain the required concentration. In order to reduce a further shearing of the DNA, a gentle inversion overnight at 0–4 °C is followed to

completely solubilize it. The purity of ctDNA sample was confirmed with the yield of A_{260}/A_{280} of approximately in the range of 1.8–1.9 (where A represents the absorbance). β–CD and dextran (Molecular weight, 20,000) were obtained from Hi Media, India. Ferrous chloride tetrahydrate, ferric chloride hexahydrate, sodium borohydride, epichlorohydrin, sodium hydroxide, ethylene diamine, and the chromenones were of analytical grade and were used without further purification. The CHRs (PC, DC, DHC, BTC, and BIC) were obtained from Sigma, India. Stock solutions of the PC, DC and DHC were prepared in ethanol and methanol is used to dissolve BTC and BIC, diluted with doubly distilled water to obtain the required concentration of test solutions. The maximum concentration of the solvents was 3 % in all the test solutions. Acetate buffer solution (10×10^{-3} mol dm^{-1}) was used to maintain the pH. The experiments were carried out at an ambient temperature of (25 ± 2) ℃. Absorption and fluorescence measurements were done against the appropriate blank solution.

Preparation of chemically modified SPIONs

Dextran (5 g, MW: 20,000) was dissolved in 20 ml double distilled water and it was sonicated for 30 minutes. Ferric chloride (0.65 g, 0.2 mol dm^{-3}) and ferrous chloride (0.51 g, 0.1 mol dm^{-3}) were dissolved in double-distilled water.[27] The sonicated dextran solution was slowly added to the ferrous-ferric solution, with constant stirring. Liquid ammonia (40 ml) was then added drop-by-drop and stirred at ≈ 0 °C. The yellow precipitate turned to dark brown at the gradual addition of ammonia. Then, it was refluxed at 80° C for 3 hours, and then cooled to room temperature, and the supernatant solution was decanted. To the dark brown precipitate, 150 ml of ethanol was added to do the aggregation of the colloidal NPs. The precipitate was centrifuged, washed, filtered, and dried to get the dextran–coated iron oxide nanoparticles. Dextran coated iron oxide (100 mg) was dissolved in 100 ml water and sonicated for 10 minutes. 0.035 gm of $NaBH_4$ and 35 ml of 2M NaOH solution were added to the above solution, sonicated for 10 minutes and then heated to 60 °C with constant stirring. 20 ml of epichlorohydrin was added to the above solution in drops under vigorous stirring

for half an hour and kept overnight to form a colloid. The colloidal solution was centrifuged and the supernatant solution was decanted to get the precipitate. Phosphate buffer solution (40 ml) was used to disperse the precipitate. Aminoethylamino-modified dextran–coated iron oxide nanoparticles was prepared by adding 35 ml of ethylene diamine to the above precipitate and keeping at 50 °C for 12 hours. It was then cooled to room temperature, filtered, dried, and characterized.

Conjugation of chromenones on chemically modified SPIONs

The conjugation of aminoethylamino–dextran–coated SPIONs and the CHRs molecule was carried out by its addition (5 mg) to 45, 60, 54, 70, 66 mg of PC, DC, DHC, BTC, and BIC (5×10^{-3} mol dm^{-3}) respectively, in suitable solvents. The mixture was stirred vigorously at 50 °C for 30 minutes and kept at room temperature. The solution was centrifuged to get the CHR–SPIONs. The absorption of the supernatant solution was measured in order to quantify the non–loaded free CHR molecules left behind in the solution. The CHR–SPIONs were filtered, crushed to get a fine powder, and characterized. The CHR–SPIONs were centrifuged at 70,000 rpm for 30 minutes. The loading efficiencies were calculated, measuring the concentration of the remaining supernatant liquid by recording their absorption using UV–Visible spectrophotometer.

Instrumentation

Absorption measurements were done using a UV–Visible spectrophotometer (V–630, Jasco, Japan) using a 1 cm path length cell. Fluorescence spectra were recorded using a spectrofluorometer (FP 750, Jasco, Japan) equipped with a 150 W xenon lamp for excitation. Both the excitation and the emission band widths were set up at 2 nm. FTIR spectra were recorded on a Perkin–Elmer spectrometer RXI, USA, using KBr pellets. Raman spectra were recorded on a Micro Raman spectrometer–800 (LabRAM HR model), France with the Argon Laser (514 nm), green colour and the voltage of 20 mW. The Scanning electron microscopy (SEM) images were recorded using a JEOL JSM 6360, Japan. A minimum accelerating voltage of 15 KeV was used to detect the presence of the possible elements by Energy

dispersive X-Ray (EDX). The diffraction pattern of the samples were recorded using a Shimadzu X-ray diffractometer, XRD 6000 (Japan) using a monochromatic X–ray beam from CuKα radiation. The particle size distribution of the magnetic nanoparticles was evaluated using dynamic light scattering measurements with a Malvern zetasizer nano ZS90, UK. The magnetization measurements were done on a Vibrating sample magnetometer, (Lakeshore 7410, US) at room temperature. X-Ray photoelectron spectra (XPS) were recorded using an Omicron (USA) instrument with an Mg Kα monochromatic X–ray source. Molecular docking was carried out using Schrodinger, in order to determine the interaction between the CHR molecule and the oligomeric part of dextran or aminoethylamino–dextran by the analysis of Glide Score and E_{model} score by uploading into Schrodinger Maestro software V 9.6 environment to get a proper binding affinity and molecular interaction (See SI 20).

Results and discussion

The loading of chromenones onto aminoethylamino–modified dextran–coated iron oxide nanoparticles, their loading efficiency, and openness for binding to DNA are studied. The magnetic behaviour, the size, and the morphology of the nanoparticles are analyzed using vibrating sample magnetometer (VSM), particle size analyser, and SEM analysis. The crystallite sizes and systems are derived using XRD.

Characterization of conjugation of chromenones onto SPIONs

Functionalization of SPIONs

The UV–Visible absorption spectrum of SPIONs show a broad absorption band with the absorption maximum, λ_{max} at 401 nm, which confirm the formation of SPIONs. The dextran–coated SPIONs show the absorption maximum at the wavelength of 218, 272, and 402 nm. Aminoethylamino modification of dextran (coated on SPIONs) leads to the appearance of the maxima viz., 270 and 402 nm. The dextran–coated and aminoethylamino–dextran–coated SPIONs were studied using FT-IR.[16] The FT-IR spectral data and spectra are given in SI 2A and SI 2B respectively. The presence of N–H stretching is seen in the case of aminoethylamino–dextran–coated SPIONs. This confirmed the aminoethylamino

functionalization of dextran on SPIONs. The surface modification results in lowering the O–H stretching frequency by ~18 cm^{-1}. In addition, the appearance of a new band at 3792 cm^{-1} shows the existence of N–H band in the chemically modified SPIONs (The attachment of aminoethylamino moiety to dextran–coated SPIONs is also confirmed by the existence of Fe 2p, N 1s, O 1s, P 2p and C 1s orbital by XPS analysis, SI 3). The Raman features of the prepared NPs are compared with Fe_3O_4 crytals and its calculated value reported with the assignment on the Raman features (SI 4).[17, 18] The surface modification of dextran–coated and aminoethylamino–dextran–coated SPIONs manifested in the electronic and vibrational properties of the material and it resulted in lowering the energy as shown by Raman spectroscopy (SI 5). The band assignments of free CHR and the loaded CHR in CHR–SPIONs are described in detail in the SI 6A and the FTIR spectra are given in the SI 6B. In general, the carbonyl group bands of the CHRs were significantly shifted in position, when attached to SPIONs. The band at ~550 cm^{-1} and ~3790 cm^{-1} are due to the Fe–O and N–H stretching of CHR–SPIONs.

Loading of chromenones onto chemically modified SPIONs

In order to understand the possibility of the strength of interaction of dextran and aminoethylamino–dextran with CHR, short oligomers of dextran with aminoethylamino end group were framed and their binding to CHR was analyzed theoretically (SI 7A and SI 7B) by the software, Schrodinger. Possible hydrogen bonds of unmodified and modified dextran with CHRs were viewed. Insignificant differences in the docking and E_{model} scores of the interaction of dextran and aminoethylamino–dextran oligomers towards the CHRs (SI 8) were observed. Reports on magnetic nanoparticles with aminoethylamino–dextran reveal a thousand times greater in vitro cellular uptake than unmodified dextran coated NPs. The dextran or the aminoethylamino–dextran shell on SPIONs lead to the decrease in the elemental proportion of Fe as analyzed by EDX spectra (SI 9A). SI 9A (a) shows K_α lines due to the presence of the elements viz., carbon, oxygen, and iron in the energy range of 0 to 10 KeV. The characteristic X–ray lines at 0.28 and 0.53 KeV correspond to the K_α lines of

carbon and oxygen respectively. The K_α (and its respective K_β lines at 7.05 KeV) and Lα for Fe are shown at 6.4 and 0.70 KeV respectively. This indicates the presence of Fe along with C and O in the SPIONs. SI 9A (a) shows the presence of chlorine ions in the energy of 2.62 KeV, characteristic of K_α transmission lines. Noticeable quantities of Phosphorous (P, K_α = 2.01 KeV) and Sodium (Na, K_α = 1.04 KeV) are observed in SI 9A (c). These may be due to the dispersion of the colloidal SPIONs in phosphate buffer saline solution. A decrease in the intensity of the number of counts per channel is inferred for the amount of Fe on the dextran coating of SPIONs (SI 9). All the EDX spectra CHR–SPIONs show the presence of the major elements like C, O and Fe, revealing that the SPIONs are intact in the complexes studied and do not separate out. BTC shows a peak at 2.31KeV due to the characteristic Ka line of the element, sulphur, present in BTC. These results confirm the loading of BTC onto CHR–SPIONs. The dispersion of the compounds in aqueous solution is shown pictorially in SI 10A. The coating of dextran or aminoethylamino–dextran on SPIONs resulted in its better dissolution. The photographic images on the free CHR and CHR after loading onto CHR–SPIONs are shown in SI 10B. The loading efficiencies of CHR onto aminoethylamino–modified dextran–coated SPIONs are calculated (Fig. 2), using equation (1), where the term complex refers to the CHR–SPIONs. The loading efficiencies are greater than 70 % in general.

$$\text{Loading efficiency (\%)} = \frac{[\text{Complex}]\text{Total} - [\text{Complex}]\text{Supernatant}}{[\text{Complex}]\text{Total}} \times 100 \qquad (1)$$

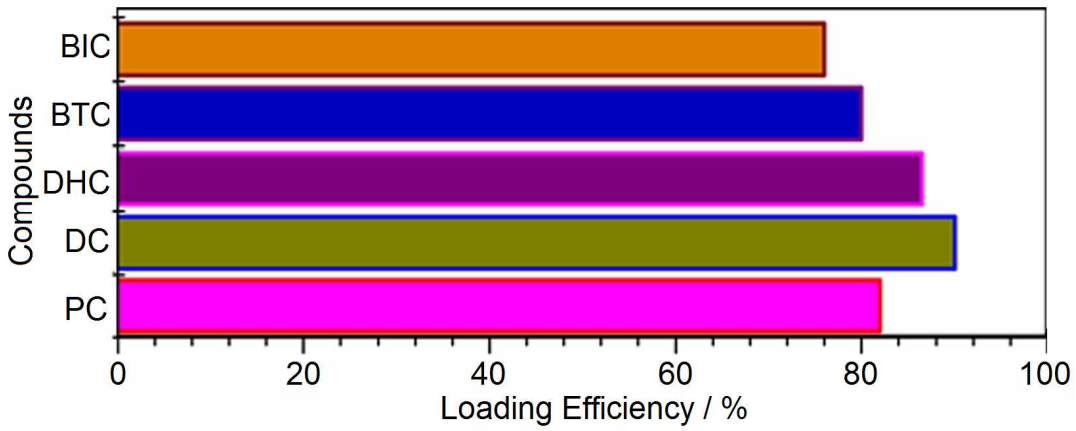

Fig. 2 Loading efficiencies of CHR onto surface modified SPIONs.

Size and magnetic properties of SPIONs

The size distributions of the SPION samples are shown in SI 11A and SI 11 B. The average particle size of the freshly prepared SPIONs was 41 nm and a surface layer (dextran coating) made it grow up in size (SI 12). The magnetizations of the aminoethylamino–dextran–coated SPIONs and the CHR–SPIONs were evaluated using VSM. The room temperature magnetic hysteresis of the compounds is shown in Fig. 3.

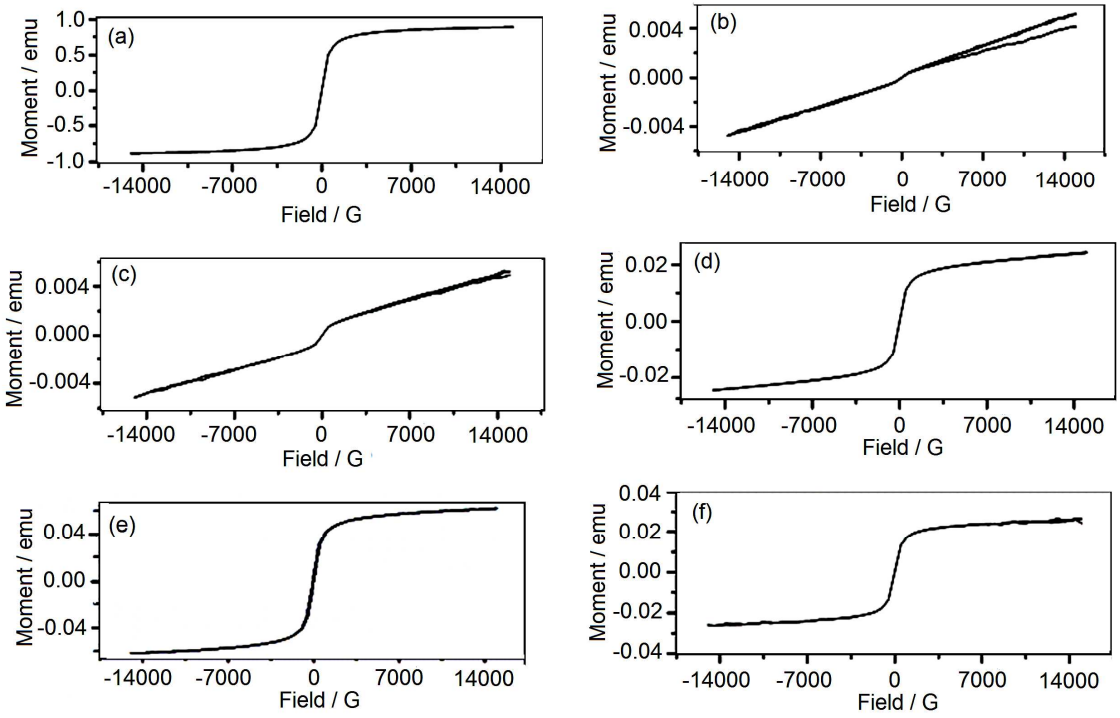

Fig. 3 Room temperature magnetic hysteresis of the compounds. (a) SPIONs, modified SPIONs loaded with (b) PC, (c) DC, (d) DHC, (e) BTC, and (f) BIC.

The SPIONs are superparamagnetic and the magnetization curve shows the absence of any hysteresis loop. The superparamagnetism is retained on surface modification of SPIONs. The magnetization curve of SPIONs passed through the origin. Perceivably, the size of the SPION core does not change much on surface modification. However, differences in saturation magnetizations (M_S) of the CHR–SPIONs are observed, which may be due to the surface effect in these samples and the role of their morphology (discussed in later section, Fig. 4). The X–Ray diffraction patterns of the SPIONs, free CHRs, and CHR–SPIONs are shown in SI

13 and SI 14 respectively. The average crystallite size is calculated using the Debye–Scherrer formula as given in equation (2),[19]

$$D = \frac{0.9\lambda}{\beta\cos\theta} \quad (2)$$

where D is the size of the crystal, λ is the wavelength of the radiation (=1.5418 Å), θ is the diffraction angle, and β is the broadening factor. The lattice strains from displacements of the unit cells about their normal positions are often produced by domain boundaries, dislocations, surfaces etc. The peak broadening due to micro–strain varies as given in equation (3), where B and ε represents the peak width and strain respectively.[20]

$$B(2\theta) = \frac{4\varepsilon\sin\theta}{\cos\theta} \quad (3)$$

The crystallite sizes and the strain in the crystals are given in SI15. The results are consistent with the observation that the SPIONs are of crystalline Fe_3O_4 structure. The peaks at various 2θ angles are in agreement with the standard card of magnetite PDF No. 01–071–6337. The noise observed at the background in the XRD pattern of aminoethylamino–dextran–coated SPIONs is due to the amorphous dextran shell. Similarly, all the CHR–SPIONs showed broad peaks due to the pronounced effect of amorphous dextran. The crystallite sizes of all the modified SPION samples fall in the range of 20 to 43 nm. Intense reflections were present at 2θ values ≈ 25° corresponding to the experimental d–spacing for iron (≈ 3.7 Å) and a high percentage of a single phase of Fe_3O_4. The crystallite size is found very close to the physical size of the SPIONs, which suggest that polycrystalline nanoparticles are not formed.

Morphology of surface–modified SPIONs

The SEM images of the free, coated SPIONs, and free CHRs are shown in Fig. 4. The colloidal SPIONs show randomly oriented irregular shaped structures due to the anisotropic dipole–dipole interactions within the microstructures.[21] Dextran coating and attachment of CHRs increase the net size of the aminoethylamino–modified dextran–coated SPIONs and, among them, quasi–linear cuboid or rod–like or spherical structures, are observed. Lateral

attraction between long chains of folded dextran sub–structures may have induced a self–

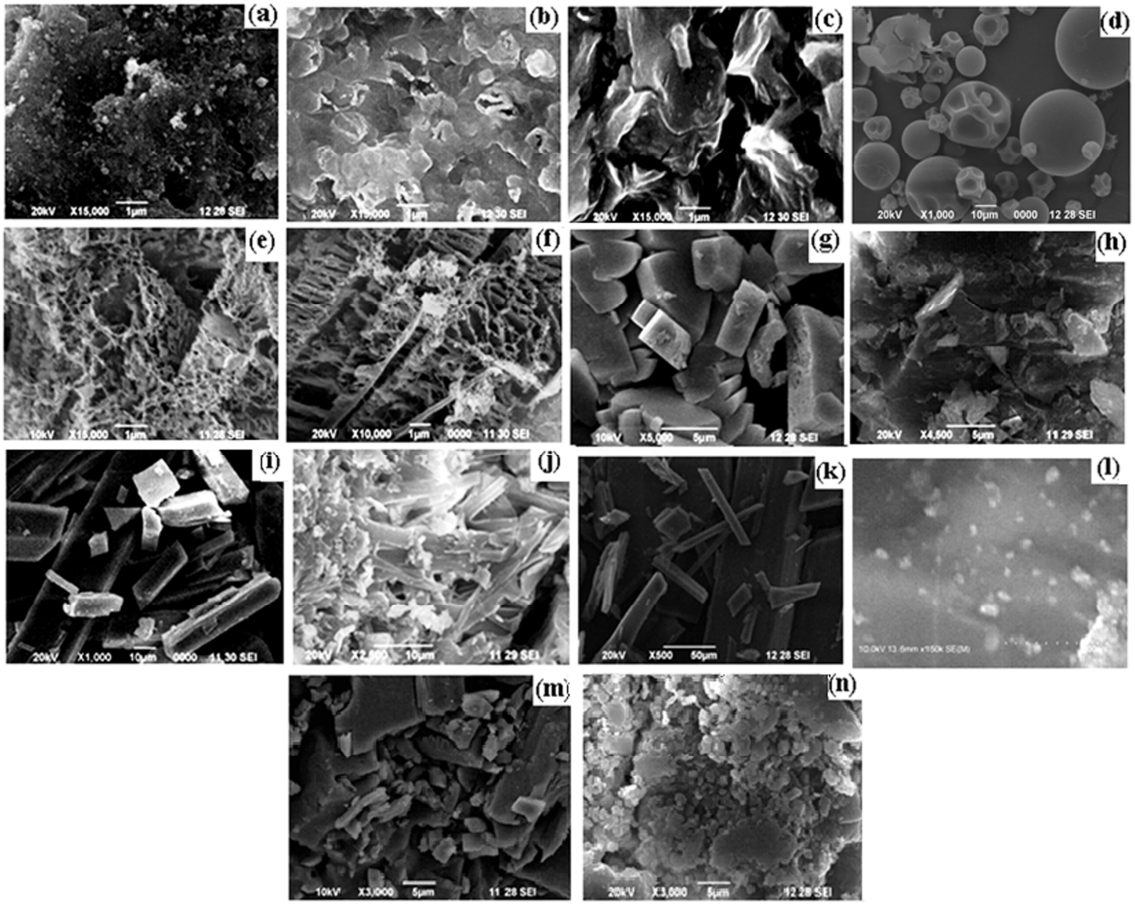

Fig. 4 SEM images of (a) SPIONs, (b) dextran–coated SPIONs, (c) aminoethylamino–dextran–coated SPIONs, and (d) dextran. CHRs and their SPIONs conjuagtes of PC (e–f), DC (g–h), DHC (i–j), BTC (k–l), and BIC (m–n).

organization and entropy minimized favoured pattern formation on the surface of SPIONs. The assembled structures belong to the micrometer scale domain, as the nanostructures grow in size with the coated layer of modified–dextran and the compounds attached on the surface. The morphology between the free CHRs and the CHR–SPIONs are different which implies that the surface of the aminoethylamino–dextran–coated SPIONs is altered at the addition of various CHRs. The ordered structures may be due to the surrounding modified dextran matrix as these structures differ in morphology from that of the naked SPIONs.

β–Cyclodextrin binding of surface–attached chromenones

β-CD is added in aliquots to solutions of CHR–SPIONs of fixed concentration and the absorption spectra of the CHR–SPIONs–β-CD titration are shown in Fig. 5. The absorption spectral data are given in Table 1.

Table 1 Absorption and fluorescence spectral data of CHR–SPIONs in water and β–CD.

CHR	CHR– SPIONs			
	Absorption wavelength (nm)		Fluorescence wavelength (nm)	
	Water	β–CD	Water	β–CD
PC	255, 321	253, 315	281, 417	281, 413
DC	286, 381	285, 381	318	316
DHC	289	287	362	363
BTC	267, 468	254, 469	511	505
BIC	272, 438	281 , 431	504	499

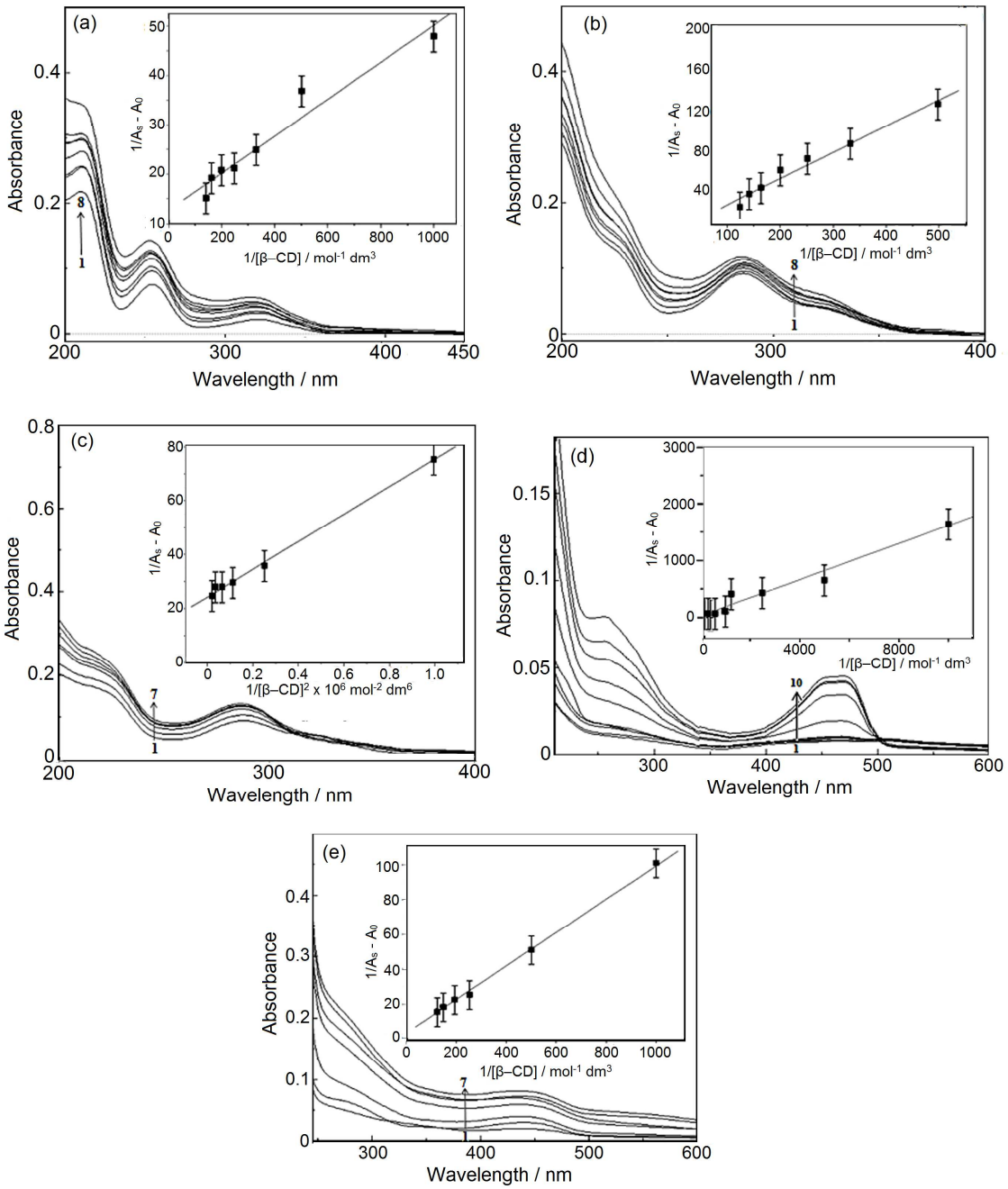

Fig. 5 Absorption spectra of the CHR–SPIONs–β-CD binding titration. (a) PC, (b) DC, (c) DHC, (d) BTC, and (e) BIC.

In general, between the free CHRs and the CHR–SPIONs compounds, there is no appreciable shift of absorption band of CHRs at the conjugation of aminoethylamino–dextran–coated SPIONs. The shifts of absorption bands of the CHR–SPIONs and those of the free, unmodified CHRs, on β–CD complex formation, are similar. The hypsochromic shift of CHR–SPIONs arises due to the change in the polarity of the environment of the

chromophores as they dislodge from the polar solvent cage of water molecules to a non–polar hydrophobic cavity of β–CD. The red shift observed in free BIC occurs probably due to the surfactant action of β–CD, with its hydroxyl groups involved in the phenomenon. The absorbance of the CHR–SPIONs gets enhanced when aqueous β–CD is added. Such hyperchromic shifts arise due to the encapsulation of the compounds by the β–CD molecule. The interaction between the hydrophobic cavity of β–CD and the non–polar moiety of the guest molecules induces a local change of environment in the system, leading to an increase in the magnitude of absorption. The evaluation of the stoichiometry and the binding constant of the β–CD–complexes of the CHR–SPIONs are done using the plots made for the following binding event:

$$\text{Host} + \text{Guest} \rightleftharpoons \text{Complex}, \tag{4}$$

$$K = \frac{[\text{Complex}]}{[\text{Host}][\text{Guest}]} \tag{5}$$

where K is the binding constant,

Using the absorption spectral data of the guest molecules (forming the host–guest complexes), the plots of $1/[\beta\text{–CD}]$ *vs.* $1/(A_S - A_0)$ of various complexes were made, following the equation (6).

$$\frac{1}{A_S - A_0} = \frac{1}{A' - A_0} + \frac{1}{A' - A_0}\frac{1}{K[\beta\text{–CD}]} \tag{6}$$

In equation (6), A_0 refers to the absorbance of each one of the CHR–SPIONs in water, A_S is the absorbance at different concentrations of the added β–CD, and A' is the absorbance at the highest concentration of β–CD. Linear plot of $1/[\beta\text{–CD}]$ *vs.* $1/(A_S - A_0)$, in the case of any of the CHR–SPIONs, leads to the inference that 1:1 host–guest complexes are formed. The binding plots made using the absorption spectral data are shown in the insets of Fig. 5. We observed a linearity pertaining to the formation of 1:1 complexes by all the CHR–SPIONs compounds except DHC, which shows a 1:2 complexation. DHC forms a 1:2 complex with aqueous β–CD in its free form also.[13] In this complex, the carbonyl group of the chromen–4–

one stands outsides the cavity of β–CD. The attachment of DHC to surface modified SPIONs does not alter the stoichiometry of the DHC–SPION–β-CD complex.

The binding of the CHR–SPIONs to β–CD is studied also using fluorescence titration (shown in SI 16). The binding plots are also shown in insets of the fluorescence spectra (SI 8). In all the cases, we observed fluorescence enhancement when β–CD was added. For a simple 1:1 host–guest complex, I/I_0 varies with the added β–CD according to the following equation (7):[22]

$$\frac{I}{I_0} = 1 + \frac{I_{max}}{(I_0-1)} \frac{K[CD]_0}{1 + K[CD]_0} \quad (7)$$

where I_{max}/I_0 is the maximum enhancement of fluorescence and K is the binding constant. A double–reciprocal plot of 1/[β–CD] vs. $1/I_{max}–I_0$ shows linearity for a 1:1 complex. In the case of 1:2 complex, the concentration of β–CD is squared and $1/[\beta–CD]^2$ is taken along the X axis and the plot is linear if the stoichiometry is 1:2. The observations in the fluorescence titration of the CHR–SPIONs against β–CD show wavelength shifts of fluorescence maxima and enhancement of fluorescence. The observations which are noteworthy in the fluorescence titration of the CHR–SPIONs against β–CD are as follows: In SPION–conjugated PC, an isoemissive point is seen in the fluorescence titration which is clearer than that observed on the β–CD–binding titration of the free PC. In the former case, we observed that the longer wavelength fluorescence band (417 nm) got quenched (or suppressed) with a corresponding enhancement of the shorter wavelength bands. A significant 4 nm blue shift on complex formation with β–CD is observed. The accommodation of guest molecules in the β–CD cavity exerts a restriction on the intra–molecular rotational and vibrational freedom of the guest molecule. Also, the local polarity experienced by the guest molecule inside the hydrophobic cavity is much smaller than that in the aqueous solution. This leads to a significant destabilization of the relative polar S_1 ground state and a smaller destabilization of the less polar S_0 ground state. This effect results further in a significantly larger $S_1 – S_0$ energy gap of the encapsulated guest molecule.[23] Hence, the fluorescence of the guest molecule is blue–shifted. The fluorescence enhancement is a consequence of the increased energy gap, which

reduces the probability of the non–radiative decay and a corresponding increase in the fluorescence quantum yield.[24] The presence of two fluorophore populations in these cases, one of which is not accessible to the quencher is evidenced by the non–linear, downward concave curve of free PC and PC conjugated to chemically modified SPIONs in fluorescence spectrum. The completion of the binding of PC (either free or conjugated to chemically modified SPIONs) with β–CD at a smaller concentration range of the host offers constraints to the accessibility of the molecules by excess β–CD molecules. These molecules show quenching of fluorescence of the 417 nm band at larger concentrations of β–CD. Deviation from linearity in the Stern–Volmer plot occurs in line with the above phenomenon (SI 16 (a)). In such cases, the Stern–Volmer constant of the binding of accessible fraction, K_a is determined (SI 16 (b)). The planar aromatic backbone of the chromenones prefers its binding to β–CD through hydrophobic interaction. There is low preference for inclusion of chromenone part of the compounds with β–CD through hydrogen bonding, if there is no hydroxyl substitution present. This is observed in the molecular docking of PC with aminoethylamino–modified dextran, in which the absence of hydrogen bonding interaction was observed. BIC showed a dual fluorescence in water, which coalesced at the step–wise addition of β–CD to form a single, broad band. This behaviour is not observed in the aminoethylamino–modified dextran–coated SPIONs–attached BIC. Instead, only a single fluorescence band is observed. This, again, may be due to the involvement of the carbonyl group of BIC in hydrogen bond formation with the aminoethylamino group. For reasons given in the preceding paragraphs on the absorption spectra of DHC, the fluorescence titration of this compound against β–CD shows a stoichiometry of 1:2. The stoichiometry and binding constants of all the host–guest complexes of the CHR–SPIONs are listed out in Table 2.

Table 2 Binding parameters of the CHR–SPIONs/Free CHR–β-CD binding.

Compd.	CHR–SPIONs				Free*			
	UV		Fluorescence		UV		Fluorescence	
	Sto.	Binding Constant	Sto.	Binding Constant	Sto.	Binding Constant	Sto.	Binding Constant
PC	1:1	3.36×10^2 M^{-1}	1:1	3.55×10^2 M^{-1}	1:1	1449 M^{-1}	-	461.61 M^{-1}
DC	1:1	14.21 M^{-1}	1:1	41.92 M^{-1}	1:2	63.97×10^4 M^{-2}	1:2	1.14×10^5 M^{-2}
DHC	1:2	4.72×10^5 M^{-2}	1:2	2.66×10^4 M^{-2}	1:2	1.44×10^4 M^{-2}	1:2	6.53×10^4 M^{-2}
BTC	1:1	45.23 M^{-1}	1:1	320.34 M^{-1}	1:1	55.72 M^{-1}	1:1	223.26 M^{-1}
BIC	1:1	36.12 M^{-1}	1:1	435 M^{-1}	1:1	69.96 M^{-1}	1:1	1.09×10^2 M^{-1}

*Refs. [11–15]

The binding constants of the complexes are calculated both from the absorption and the fluorescence binding titrations. From the reported binding constants of the free CHR–β–CD complexes, the binding constants of the CHR–SPIONs show a marked decrease in their magnitudes, with the stoichiometry remaining unaltered. The binding constant is generally dependent on the fit of the guest molecule inside the β–CD cavity as well as its polarity, and any other type of bonded interaction in the complex. The fluorescence enhancement depends only on the polarity, and the degree of sensitivity to polarity is different for different guest molecules. Since the polarity experienced by the native compounds is different from that of the CHR–SPIONs, there occurs a different rate of enhancement of fluorescence. From the observations in the absorption and fluorescence titrations, it is found that the CHR–SPIONs, bind to β–CD and hence the CHR moieties are locally accessible from outside the modified dextran shell. However, the binding constant values are decreased in magnitude, implying that the strength of binding is altered. This again is a reflection on the accessibility of CHR moieties on the surface of SPIONs by β–CD.

Openness of chromenones loaded on chemically modified SPIONs for binding to DNA

Fig. 6 shows the absorption spectral changes of CHRs on the addition of ctDNA. In general, CHR–SPIONs display hyperchromic shifts of absorption bands with little blue shifts (SI17) from native chromenones.[11–15] The longer wavelength absorption band of SPIONs–attached PC (321 nm) appears 3 nm blue–shifted than the same band of free PC. This absorption band shows a hypochromic shift on the addition of ctDNA to free PC, whereas there is a

hyperchromic shift of the absorption of SPION–attached PC on DNA addition (Fig. 6 (a)). The shorter wavelength band (255 nm) shows a hyperchromic shift without significant shift of absorption wavelength due to DNA binding. The hyperchromic shift of the longer wavelength band suggests that the same PC: DNA stoichiometry is preserved during the binding process. The hypochromic shift of the 255 nm band implies that there is an additional mode of binding in free PC. Hydrogen bonding and electrostatic interaction also may operate during the binding of free PC to DNA. In the case of the binding of SPION–attached PC onto DNA, the binding constant (7.33×10^5 M^{-1}) (SI18) is larger. SPION–attached BIC shows a hypochromic shift on binding to DNA (Fig. 6 (e)). A small red shift of ~3 nm is also observed due to the decrease of polarity in the local environment of DNA.

The compounds other than SPION–attached PC and BIC display hyperchromic shifts of absorption bands with little blue shifts. Single isosbestic points are absent in some of the compounds, indicative of the absence just one mode of binding. In general, most of the compounds display absorption characteristics similar to unmodified native compounds, on DNA binding. There is a general decrease in the binding strength of the CHR–SPIONs, from the binding strengths of native CHRs. However, larger binding constant values of SPION–attached DC, is observed on DNA binding, compared to their corresponding native forms. An increase in the binding constant value is an indication that the SPION attachment of CHRs does not hinder their binding to DNA. A decrease in the binding constant in the other compounds may be due to the lesser availability of the compounds for binding, being in a molecular crowded environment. Moreover, the higher molecular weight dextran does not trap the aminoethylamino–dextran–coated SPIONs–attached CHR compounds into their possibly coiled strands. Instead, the CHRs are available on the surface of the aminoethylamino–dextran–coated SPIONs in a way they remain free to bind to DNA.

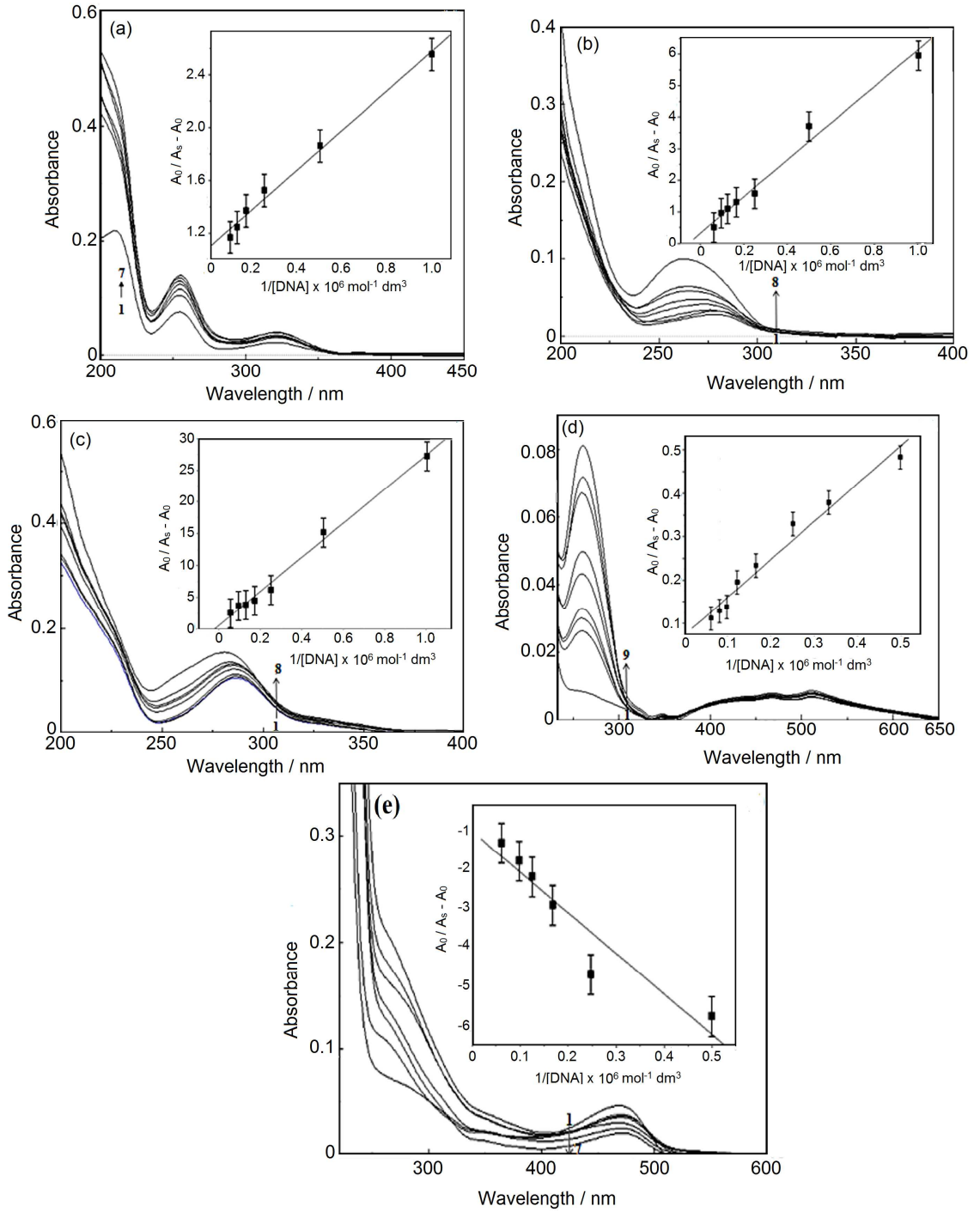

Fig. 6 Absorption spectra of the binding titrations of CHRs–DNA interactions. (a) PC, (b) DC, (c) DHC, (d) BTC, and (e) BIC.

The binding of CHR–SPIONs to DNA is also studied using fluorescence spectroscopy (SI 19). The enhancement of fluorescence is observed for CHRs conjugated to modified SPIONs except BIC binding to DNA. This enhancement occurs due to the stacking of the planar aromatic backbone of chromenones between the adjacent base pairs of DNA. BIC show

quenching of fluorescence on the addition of aliquots of DNA keeping the concentration of the fluorophores fixed. The quenching of fluorescence is an indication of the binding interaction between each of these compounds and DNA. The Stern–Volmer constant (K_{SV}) is calculated from the fluorescence titration data using the following equation (8),[25]

$$\frac{I_0}{I} = 1 + K_{sv}[Q] \quad (8)$$

where I_0 and I are the intensities of fluorescence of the SPION–attached BIC in the absence and the presence of DNA. The K_{SV} in this case is calculated as 1.27×10^5 M^{-1}. The compounds PC, DC, DHC, and BTC of CHR–SPIONs show enhancement of fluorescence at the addition of DNA. These show that the binding of these SPION–attached CHRs to DNA takes place. This is thought to occur due to the change of micro–environmental polarity through the removal of water molecules by intercalation.[26] Hence, the surface–loaded chromenones are able to bind to DNA, although doing so with a lesser binding constant values than the free CHR–DNA binding.

Conclusions

The loading of chromenones onto aminoethylamino–dextran–coated superparamagnetic iron oxide core–shell nanoparticles, and the openness of chromenones for their binding to β–cyclodextrin and DNA are studied in terms of their binding strength and stoichiometry. Enhancement of fluorescence of chromenones, conjugated with chemically modified superparamagnetic iron oxide nanoparticles, is observed on binding to β–cyclodextrin, except in the case of flavanone. There are two fluorophore populations of flavanone, one of which is not accessible to the quencher. 1:2 inclusion complex formation is observed in Naringenin conjugated to superparamagnetic iron oxide nanoparticles. The hydrophobicity of the chromenone moiety of the compounds plays a significant role in binding to DNA. Enhancement of fluorescence is observed on the DNA binding of chromenones conjugated to superparamagnetic iron oxide nanoparticles, except Coumarin 7. Dextran coating retains the superparamagnetic behavior of iron oxide nanoparticles. The chromenones get loaded onto the shell of aminoethylamino-dextran, with the involvement of hydrogen bonding. This

loading, weaker than covalent bonding, is best for the delivery of drugs. The chromenones are on the surface of the modified dextran shell, rendered accessible by β–cyclodextrin during the formation of inclusion complexes. The strengths of their β–cyclodextrin complexes are lesser when compared to those of the free chromenones. The chromenones–loaded superparamagnetic iron oxide nanoparticles are intact and do not undergo precipitation within the studied concentration range. The surface–loaded chromenones are able to bind to DNA, although doing so with a lesser binding constant values than the free chromenones –DNA binding. The results suggest the availability of the compounds on the surface of superparamagnetic iron oxide nanoparticles, and are accessible by DNA for binding.

Acknowledgements

We thank the Chancellor Dr. Paul Dhinakaran, the Vice–Chancellor Dr. Sundar Manoharan, for setting up the new research lab, and our Director Dr. Daphy Louis Lovenia, for providing necessary facilities.

Notes and references

1 Y. Zhu, C. Tao, *RSC Adv.*, 2015, 5, 22365–22372.

2 M. Morteza, S. Shilpa, W. Ben, L. Sophie, S. Tapas, *Adv. Drug Deliv. Rev*. 2011, **1–2**, 24–46.

3 J. M. Perez, A. Asati, S. Nath, C. Kaittanis, *Small* 2008, **4**, 552–556.

4 A. Jordan, R. Scholz, P. Wust, H. Schirra, T. Schiestel, H. Schmidt, R. Felix, *J. Magn. Magn. Mater.* 1999, **194**, 185–96.

5 V. P. Torchilin, *Biopolym.* (*Pept. Sci*), 2008, **90**, 604–10.

6 H. Cho, D. Alcantara, H. Yuan, A. R. Sheth, H. H. Chen, P. Huang, S. B. Andersson, D. E. Sosnovik, U. Mahmood, L. Josephson, *ACS Nano* 2013, **7**, 2032–2041.

7 W. Saenger, *Angew. Chem. Int. Ed. Engl.,* 1980, **19**, 344–362.

8 J. Szejtli, *Cyclodextrin Technology*, Kluwer Academic Publishers, Doedrecht, Netherlands, 1988.

9 Y. Sameena, N. Sudha, S. Chandasekaran. I. V. M. V. Enoch, *J. Biol. Phys*., 2014, **40**, 347–367.

10 I. V. M. V. Enoch, M. Swaminathan, *J. Chem. Res.*, 2006, **8**, 523–526.

11 S. Chandasekaran, Y. Sameena, I. V. M. V. Enoch, *Turk. J. Chem*. 2014, **38**, 725–738.

12 Y. Sameena, I. V. M. V. Enoch, *J. Lumin*. 2013, **138**, 105–116.

13 Y. Sameena, I. V. M. V. Enoch, *AAPS Pharma. Sci. Tech.* 2013, **14**, 770–781.

14 S. Chandasekaran, Y. Sameena, I. V. M. V. Enoch, *J. Mol. Recognit*. 2014, **27**, 640–652.

15 S. Chandasekaran, Y. Sameena, I. V. M. V. Enoch, *J. Incl. Phenom. Macro. Chem.* 2014, **81**, 225–236.

16 G. Du, Z. Liu, X. Xia, L. Jia, Q. Chu, S. Zhang, *Nanoscience* 2006, **11**, 49–54.

17 C. S. S. R. Kumar, *Raman Spectroscopy For Nanomaterials Characterisation*, Springer–Verlag, Berlin, Heidelberg, 2012, 1–646.

18 H. Monika, *Geophys. J. Int*. 2009, **177**, 941–948.

19 J. I. Langford, A. J. Wilson, *J. Appl. Cryst.,* 1978, **11**, 102–113.

20 A. R. Bushroa, R. G. Rahbari, H. H. Masjuki, M. R. Muhamed, *Vacuum* 2012, **86**, 1107–1112.

21 J. Liu, E. M. Lawrence, A. Wu, M. L. Ivey, G. A. Flores, K. Javier, J. Bibette, J. Richard, *Phys. Rev. Lett*. 1995, **74**, 2828–2831.

22 A. Munoz de la Pena, F. Salines, M. J. Gomez, M. A. Acedo, M. Sanchez Pena*, J. Incl. Phenom. Mol. Rec. Chem.*, 1993, **5**, 131–143.

23 B. D. Wagner, *The Effects of Cyclodextrins on Guest Fluorescence, in Cyclodextrin Materials: Photochemistry, Photophysics, and Photobiology*. Ed.: A. Douhal, Elsevier, 2006, p. 41.

24 R. Englman, J. Jortner, *Mol. Phys*. 1970, **18**, 145–64.

25 J. R. Lakowicz, J. R. *Principles of Fluorescence Spectroscopy*, 3rd Edition, Springer, 2006.

26 S. Chandrasekaran, Y. Sameena, I. V. M. V. Enoch, *Aust. J. Chem.*, 2014, **67**, 256–265.

27 A. – H. Lu, E. L. Salabas, F. Schuth, *Angew. Chem. Int. Ed*., 2007, **46**, 1222–1244.